Research Article | Vol. 11, No. 1 / 1 January 2021 / Optical Materials Express 80
Optical Materials EXPRESS

Intensity-modulated directional torsion sensor based on a helical fiber taper

QI GUO,[1] YONG-QIN ZHU,[2] TIAN-QI SHAN,[1] XUE-PENG PAN,[1] SHAN-REN LIU,[1] ZHAO-KANG XUE,[1] ZHONG-MING ZHENG,[3] CHAO CHEN,[3] AND YONG-SEN YU[1,*]

[1]*State Key Laboratory of Integrated Optoelectronics, College of Electronic Science and Engineering, Jilin University, 2699 Qianjin Street, Changchun 130012, China*
[2]*Beijing Microelectronics Technology Institute, Beijing 10076, China*
[3]*Changchun Institute of Optics, Fine Mechanics and Physics, Chinese Academy of Sciences, Changchun 130033, China*
[*]*yuys@jlu.edu.cn*

Abstract: A novel intensity-modulated directional torsion sensor based on a helical taper is proposed and experimentally demonstrated. The tapers are fabricated in standard single-mode fiber by electric-arc discharge, and by rotating one side fiber simultaneously. Experimental results show that the intensity of transmission peak changes inversely when the helical taper is twisted in clockwise and counterclockwise, respectively. The maximum torsion sensitivity can reach -0.484 dB/(rad/m) in the twist rate ranges from -10.67 rad/m to 0 rad/m. Additionally, this torsion sensor is almost insensitive to temperature, which solves the problem of torsion-temperature cross sensitivity greatly. The novel torsion sensor provides a promising candidate for the applications that require accurate rotation, such as civil engineering, the automotive industry, and security monitoring of buildings.

1. Introduction

Optical fiber sensors have the advantages of small size, light mass and anti-electromagnetic interference, which have attracted lively interest in many fields [1,2]. For example, a holographic control method for light propagating in complex media was proposed recently, and it enabled multimode fibers to be used as an ultra-narrow imaging tool [3]. In addition, the multimode optical fiber transmission based on deep learning networks has also been studied [4]. Torsion is an important mechanical parameter that reflects the stress state and internal injury of the monitored structure, and the torsion sensors can be embedded in engineering structures for internal strain detection [5] and structural health monitoring [6,7]. Furthermore, in the past decades, the highly sensitive and directional torsion measurements using an optical fiber sensor have been employed in many applications, such as robotics, civil engineering [8], and automotive industry. For example, the wind turbine blades are deformed after a long period of abrasion, resulting in reduced efficiency. Hence, structural monitoring of the blades is necessary to detect fatigue failure and production optimization of the wind turbines, which can be greatly achieved by measuring the twist of blades [9]. In recent years, the torsion sensors based on various fiber structures have been investigated [10], such as FBGs [11,12], LPFGs [13–15], and Mach-Zehnder interferometers (MZIs) [9,16,17]. In 2017, Ping Lu's research group successfully fabricated a novel torsion sensor with relatively high sensitivity, and it is based on a tapered sandwich structure [18]. Moreover, its torsion sensitivity reached 0.12 dB/° and it solved the problem of temperature cross sensitivity by power demodulation. Recently, Yi-Ping Wang's research team reported a novel directional torsion sensor, which is in a helical photonic crystal fiber with an embedded liquid rod waveguide [19]. This torsion sensor can distinguish the rotational direction and had a relatively high sensitivity that up to 0.208 nm/(rad/m). However, as far as we know,

#411139 https://doi.org/10.1364/OME.411139
Journal © 2021 Received 28 Sep 2020; revised 27 Nov 2020; accepted 30 Nov 2020; published 8 Dec 2020

Optical Materials EXPRESS

many torsion sensors so far reported can only measure the twist rate, which can't distinguish the rotational direction [18,20]. Additionally, there are also some torsion sensors, whose are complicated to fabricate and costly [17,21], and the others are sensitive to temperature that have the problem of cross sensitivity in practical applications [22,23].

In this work, a novel directional torsion sensor is proposed. Firstly, the torsion sensor is fabricated by an electric-arc discharge method in single mode fiber (SMF), which the fabrication process is simple and the cost is low. And by introducing an initial helical structure when pulling the taper, the torsion sensor can measure twist rate and distinguish its rotational direction simultaneously. Furthermore, because the size of the helical taper is only a few hundred micrometers, the torsion sensor is almost insensitive to temperature, which solves the problem of torsion-temperature cross sensitivity greatly.

2. Experiment process

2.1. Experimental setup

The device diagram of fabricating the helical taper is demonstrated in Fig. 1(a). This helical taper structure was fabricated in standard single mode fiber (SMF-28e, Corning.) by an electric-arc discharge method. Firstly, the fiber with coating removed was straightly placed in the V-groove of a fusion splicer (Ericsson FSU-995PM), and fixed by the fiber clamps. Then, one user-defined tapered program was selected. What's more, the discharge time and current must be chosen appropriately. If the current is too small, the taper can't be drawn, and if it is too large, the taper is easily blown. In addition, the discharge time must be also greatly controlled to obtain a better spectrum. By continuously researching the discharge time and current, the optimal parameters were obtained as follows: discharge time = 12s, discharge current = 10mA. Finally, when the tapered program started, the fiber clamp at the right end was rotated 360° simultaneously.

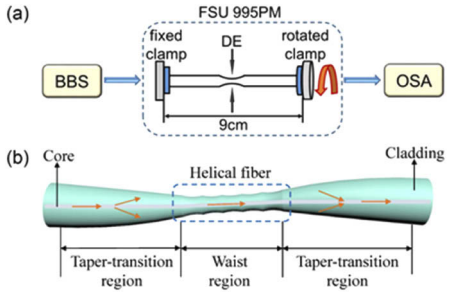

Fig. 1. (a) The device diagram of fabricating this helical taper. (b) The schematic diagram of the fabricated helical taper.

During the fabrication of this helical taper, its spectra are monitored in real time by the experimental setup shown in Fig. 1(a). A light source (Superk Compact, NKT Photonics, Inc.) with broadband of 500nm-2400nm outputs supercontinuous light. And the transmission spectrum of this helical taper is recorded by an optical spectrum analyzer (OSA) (Yokogawa AQ6370B). The Fig. 1(b) is the schematic diagram of the helical taper, and it can be clearly seen that the helical taper is slightly micro-bend due to the perturbation of applied 360° rotational force. When the light propagates along the micro-bend region, a portion of core mode is coupled to the cladding, resulting in bending loss. Additionally, in the taper waist region, there is a distinct helical shape due to the rotation when pulling.

The Fig. 2(a) is the transmission spectrum of this helical taper. Among them, the dip A and dip B are labeled for the following torsion test. Then, the transmission spectrum is subjected to fast Fourier transform (FFT), and the spatial frequency spectrum is obtained. As demonstrated

Optical Materials EXPRESS

in Fig. 2(b), there are two dominant peaks, which located at 0.00998 nm^{-1} and 0.0160 nm^{-1}, respectively. These two frequency peaks indicate that there are mainly two excited cladding modes, and they interact with core mode, forming interference fringes. In order to explain the coupling process and spectrum composition of helical fiber taper mode more clearly, the coupling of two cladding modes and three cladding modes with the core mode is simulated by MATLAB software, as shown in Fig. 2(c) and (d). It can also be seen from the FFT spectrum that there are many spectrum components, and two strong cladding modes are mainly coupled with the core mode.

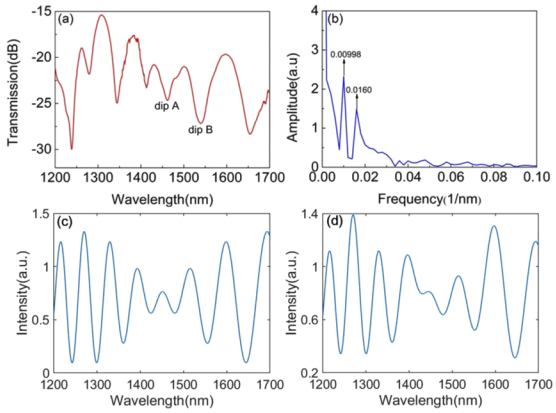

Fig. 2. (a) Transmission spectrum of this helical taper. (b) FFT spectrum of the corresponding transmission spectrum. (c) Simulation of coupling between two cladding modes and core mode. (d) Simulation of coupling between three cladding modes and core mode.

2.2. Sensing principle

When the light propagates along the helical taper, as shown in Fig. 1(b), in the micro-bend region, a portion of core mode is coupled to cladding. And in the latter taper-transition region of the helical taper, the cladding mode is recoupled back, interfering with the core mode. Therefore, the sensing principle of this helical taper is a Mach-Zehnder interferometer. Additionally, the polarization state of input light will change at this helical taper [23], and the thin taper waist will increase the evanescent field, which improves the torsion sensitivity. The intensity of output light is expressed as:

$$\mathrm{I}_{out} = I_{co} + I_{cl} + 2\sqrt{I_{co}I_{cl}}\cos(\Phi) \tag{1}$$

where I_{co} and I_{cl} are the intensity of core and cladding separately, and Φ is the phase difference of them. Since the effective refractive index of core and cladding is different, the light has different propagation speed in them, which generates a phase difference after a certain distance of transmission. And the phase difference Φ can be expressed as:

$$\Phi = (2\pi\Delta n_{eff}L)/\lambda \tag{2}$$

where Δn_{eff} is effective refractive index difference of core mode and cladding mode, L is the length of this interferometer, and λ is wavelength of the input light. When $\Phi=(2m+1)\pi$, where m is a positive integer, there are a series of attenuation peaks in the wavelength ranges of 1200 nm-1700 nm, as demonstrated in Fig. 2(a).

When the torsion test is performed, one end of the fiber is fixed and the other is free to rotate, applying transverse shear to the helical taper. The cross-section of the fiber is subjected to a shear strain that can be expressed as [24]: $\varepsilon = (D\theta)/(2L_0)$, where D is diameter of the single mode

Optical Materials EXPRESS

fiber, θ is the twist angle, and L_0 is the length between two fiber clamps. The applied twist causes the elastic-optical effect, which in turn leads to the circular birefringence. When the helical taper is twisted, the polarization state of the input light changes with twist angle, which can be written by a Jones matrix F_L [25]:

$$F_L = \begin{bmatrix} \cos\eta - i\frac{\delta_L}{2}\frac{\sin\eta}{\eta} & \frac{\delta_C}{2}\frac{\sin\eta}{\eta} \\ -\frac{\delta_C}{2}\frac{\sin\eta}{\eta} & \cos\eta + i\frac{\delta_L}{2}\frac{\sin\eta}{\eta} \end{bmatrix} \tag{3}$$

where δ_L is the phase difference of the inherent linear birefringence in a single mode fiber, and δ_C is a phase term of the circular birefringence caused by the twist. In addition, $\delta_L = \Phi = (2\pi\Delta n_{eff}L)/\lambda$, $\delta_C = 2(1-g)\cdot\theta$, and $\eta = \sqrt{\left(\frac{\delta_L}{2}\right)^2 + \left(\frac{\delta_C}{2}\right)^2}$. For a standard single mode fiber, the difference of linear birefringence Δn_{eff} is about 10^{-7}, which can be considered equal to 0, and the constant g is about 0.16 [26]. Therefore, the Jones matrix F_L is simplified to:

$$F_L = \begin{bmatrix} \cos\frac{\delta_C}{2} & \sin\frac{\delta_C}{2} \\ -\sin\frac{\delta_C}{2} & \cos\frac{\delta_C}{2} \end{bmatrix} = \begin{bmatrix} \cos(0.92\theta) & \sin(0.92\theta) \\ -\sin(0.92\theta) & \cos(0.92\theta) \end{bmatrix} \tag{4}$$

And the output light field vector is [27]: $I_{out} = F_L \times I_{in}$, where I_{out} is the output light intensity, and I_{in} is the incident light intensity. Thus, the output light intensity is only related to the twist angle θ.

As shown in Fig. 1(a), when we fabricated the helical taper structure, an original twist angle θ_0 was introduced. Hence, the actual twist angle is equal to $(\theta_0 \pm \theta)$, the "+" and "−" means applied twist in clockwise (CW) and counterclockwise (CCW) direction when conducted the torsion test. Among them, the clockwise represents the same direction as the fabricated helical taper, as the direction that marked in Fig. 1(a), and the counterclockwise indicates the opposite rotational direction when performed a torsion test. Therefore, during the following torsion test, when the helical taper is twist in opposite directions, the intensity of transmission peaks changes inversely.

3. Results and discussion

3.1. Torsion sensing

The torsion characteristic of the helical taper was investigated experimentally. And the experimental device diagram for torsion test is shown in Fig. 3. Firstly, the helical taper structure was placed carefully, and ensure that it is not bend with no additional tension. Then the one end fiber clamp was fixed and the other can be rotated in clockwise and counterclockwise direction, respectively. Here, the clockwise means the twist direction when fabricated the helical taper, as the direction that shown in Fig. 1(a). And the opposite direction is defined as the counterclockwise. Finally, set the rotational angle step to 5°, which corresponding to a twist rate step of 0.970 rad/m. The twist rate is defined as: $\tau = \alpha/L_0$, where α is the twist radian of the fiber, and L_0 is the length between the two fiber clamps, which is 9cm. Here, compared with twist angle, the twist rate can more accurately represent the shear force applied on the helical taper.

Using an arc discharge method, the helical taper with a waist diameter of 54.6 um was fabricated firstly. The Fig. 4 and Fig. 5 are the torsional experimental results of this structure. Among them, the Fig. 4(a) demonstrates variation of transmission spectra with increasing of twist rate in clockwise direction. It can be clearly observed that with the increasing of twist rate from 0 rad/m to 10.67 rad/m, the transmission intensities are both increase of dip A and dip B, which indicates by these two red arrows. Additionally, the Fig. 4(b) demonstrates the shift of transmission spectra with the twist rate ranging from -10.67 rad/m to 0 rad/m. And with the increasing of twist rate in counterclockwise, transmission peaks intensities are decrease, as

Optical Materials EXPRESS

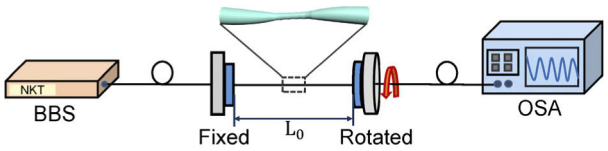

Fig. 3. The experimental device diagram for torsion test.

shown by the blue arrows, which has opposite variation compared to clockwise twist. To the best of our knowledge, the polarization state of incident light propagating through this helical taper can be described by a Jones matrix F_L [28]. And according to the Eq. (4), as the twist applied on the fiber, the polarization state of incident light changes, leading to the variation of transmission dip intensity. In addition, because there is a 360° pre-twist when fabricated this helical taper, the intensity varies conversely in clockwise and counterclockwise torsional test. Furthermore, as shown in Fig. 4, the birefringence change caused by the twist is too small [29], the wavelengths of these two peaks hardly shift. Therefore, according to the intensities of transmission peaks have contrary variation when the helical taper is twisted in opposite directions, we can identify rotational direction. Moreover, this torsion sensor adopts the method of intensity modulation, which does not require expensive spectrometer, so the cost is greatly low in practical applications. Helical fiber tapers are fabricated by applying torsion stress in a clockwise direction. When the stress is applied in the clockwise direction, the helical degree increases and the optical loss increases. Due to the elastic-optical effect, the refractive index will change greatly and the spectral wavelength will shift. When counterclockwise stress is applied, the helical degree decreases, which is equivalent to unwinding the helix, and the optical loss decreases. At this time, the elastic-optical effect is weak, the change of refractive index is small, and the change of spectral wavelength is not obvious.

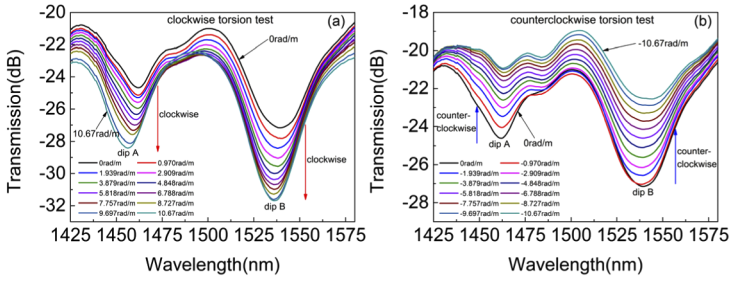

Fig. 4. (a) Transmission spectrum of dip A and dip B changes with the twist rate increasing in clockwise. (b) Transmission spectrum changes with the twist rate increasing in counterclockwise.

The Fig. 5 demonstrates the relationship of transmission intensity and twist rate. It can be observed that with the changing of twist rate, the intensity variation of dip A and dip B has a similar trend. Then by linearly fitting the experimental data, the torsion sensitivity of these two peaks can be obtained. In addition, compared with dip A, the dip B has a better linearity and a higher torsion sensitivity. Moreover, the performance of transmission dips is closely related to the mode coupling between core mode and the excited cladding mode [17], as well as the optical anisotropy in twisted fiber [9]. And the dips in different locations are mainly determined by the order of excited cladding mode. Thus, the dip B is formed by a relatively higher order cladding mode interacting with core mode, which has greater sensing performance. The highest sensitivity is achieved when the dip B in counterclockwise twist measurement, which reaches up

Optical Materials EXPRESS

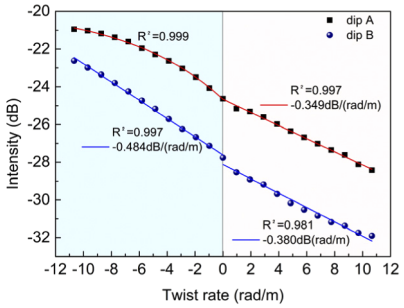

Fig. 5. The relationship between the intensity of two transmission peaks and twist rate.

to -0.484 dB/(rad/m) with the R-square of 0.997. Furthermore, the linearity is closely related to the twist angle, such as in the Refs. [28] and [29], with the twist angle ranging from 0° to 360°, the intensity of transmission dip varies periodically with the twist angle as a sine-like function. Here, since the waist of the fabricated helical taper is thin, its mechanical strength is weak, and the applied twist angle is only between 0° and 55°. Therefore, in this small twist range, the transmission intensity and twist rate show better linearity [9]. Additionally, the torsion sensitivity is different for clockwise and counterclockwise measurements, and this can be explained for the following reasons. On the one hand, due to the twist-induced optical anisotropy of fiber [30] and the applied pre-twist during the fabrication of helical taper, the structure exhibits to be asymmetrical, resulting in the different sensitivity in clockwise and counterclockwise. On the other hand, the applied twist also induces the circular birefringence of fiber [31], which makes the difference of torsion sensitivity in clockwise and counterclockwise to a certain extent.

In order to improve the completeness and persuasiveness of the torsion sensing, other waist diameters of the helical taper were also fabricated and tested. The Fig. 6 is experimental results of torsion test. And compared with the sensing structure with a waist diameter of 54.6um that mentioned above, their dip intensity has the same variation law, which is increase in clockwise twist and decrease in counterclockwise. From the insets of Fig. 6, the torsion sensitivities of these two structures can be obtained. Among them, the sensitivity with waist of 62.5um are -0.329 dB/(rad/m), and it is -0.213 dB/(rad/m) with the waist diameter of 66.9um. Additionally, comparing the results of these three different waist diameters, it can be found that the thinner taper waist has higher sensitivity. This is because the structure suffers more twist force if the waist is thinner, leading to greater deformation. However, a too thin taper waist will greatly reduce the mechanical strength of the structure, so reasonable waist parameters should be chosen when fabricating.

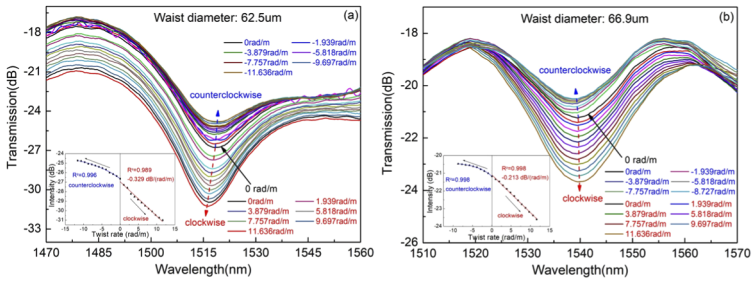

Fig. 6. (a)The variety of transmission spectra with the waist diameter of 62.5um. (b)The shift of transmission spectra with the waist diameter of 66.9um. Insets: The relationship between intensity and twist rate.

Optical Materials EXPRESS

3.2. Temperature sensing

Lately, the temperature response of the helical taper was also researched. Firstly, the helical taper was fixed in the center of a heating table with a temperature resolution of 1 °C, and in order to ensure the accuracy of the temperature test, a cover was placed on the heating table to maintain the temperature at the set values. With the temperature gradually increasing from room temperature (17°C) to 100°C, the transmission spectrum was recorded by using a spectrometer. As shown in Fig. 7, with the increasing of temperature, the intensities of dip A and dip B both hardly change. The inset plots the relationship between temperature and transmission intensity. And from the inset, the temperature sensitivities of dip A and dip B can be obtained that are 0.00102 dB/°C and 0.00039 dB/°C separately. Compared to the torsion sensitivity of the helical taper, these temperature sensitivities are greatly low, which can be neglected for the torsion measurement. Therefore, we can consider that the helical taper structure is almost insensitive to temperature, and this effectively solves the problem of torsion-temperature cross sensitivity in practical applications.

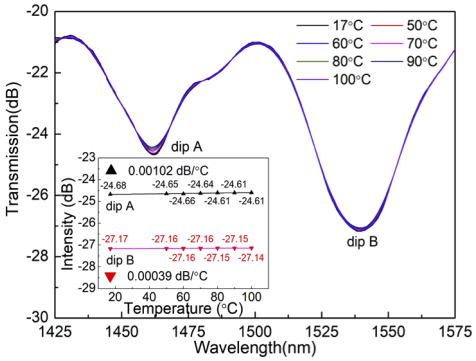

Fig. 7. The transmission spectrum changes with different temperatures. Inset: The transmission intensity changes with temperature.

The main reason why helical fiber taper is not sensitive to temperature is that when the ambient temperature changes, the refractive index of the optical fiber material changes due to the thermo-optical effect and thermal expansion effect of the material, which causes the shift of the sensor's transmission spectrum wavelength. The center wavelength shift of the m-order interference fringe caused by the change of external temperature can be expressed as follows [32–34]:

$$\Delta\lambda_{\mathrm{m}} = (\alpha + P_t)\lambda_m \Delta T \tag{5}$$

Where P_t is the difference of effective refractive index between the two modes when the external temperature changes, α is the thermal expansion coefficient of the material, and ΔT is the change of the external temperature. Because the coefficient of thermal expansion of quartz is very small, from room temperature to 100 °C, the effect of thermal expansion caused by temperature change is very small, which leads to little influence on the change of transmission mode, and the change of P_t caused by temperature change is approximately 0. Therefore, helical fiber taper is insensitive to temperature, which avoids the cross-sensitivity problem when temperature and torsion are measured simultaneously.

4. Conclusion

We propose a novel torsion sensor based on a helical taper. And this helical fiber taper is fabricated by a method of electric-arc discharge of a fusion splicer, which the fabrication process is simple and the cost is greatly low. The experimental results of torsion sensing indicate that when the

Optical Materials EXPRESS

structure is twisted in different directions, the intensity of transmission peaks varies inversely. Therefore, the torsion sensor can measure twist rate and distinguish its rotational direction simultaneously, and the maximum sensitivity can reach -0.484 dB/(rad/m). Additionally, the helical taper is almost insensitive to temperature, which solves the problem of torsion-temperature cross sensitivity greatly.

Funding

National Natural Science Foundation of China (91860140, 62090061, 61874119, 61905244); Science and Technology Development Project of Jilin Province (20180201014GX).

Acknowledgments

This work was supported by the National Natural Science Foundation of China (91860140, 62090061, 61874119, 61905244) and the Science and Technology Development Project of Jilin Province (20180201014GX).

Disclosures

The authors declare that there are no conflicts of interest related to this article.

References

1. Z. M. Zheng, Y. S. Yu, X. Y. Zhang, Q. Guo, and H. B. Sun, "Femtosecond laser inscribed small-period long-period fiber gratings with dual-parameter sensing," IEEE Sensors J. **18**(3), 1100–1103 (2018).
2. S. M. Nalawade, S. S. Harnol, and H. V. Thakur, "Temperature and strain independent modal interferometric torsion sensor using photonic crystal fiber," IEEE Sensors J. **12**(8), 2614–2615 (2012).
3. S. Turtaev, I. T. Leite, T. Altwegg-Boussac, J. M. P. Pakan, N. L. Rochefort, and T. Cizmar, "High-fidelity multimode fibre-based endoscopy for deep brain in vivo imaging," Light: Sci. Appl. **7**(1), 92 (2018).
4. B. Rahmani, D. Loterie, G. Konstantinou, D. Psaltis, and C. Moser, "Multimode optical fiber transmission with a deep learning network," Light: Sci. Appl. **7**(1), 69 (2018).
5. H. P. Wang, L. Z. Jiang, and P. Xiang, "Improving the durability of the optical fiber sensor based on strain transfer analysis," Opt. Fiber Technol. **42**, 97–104 (2018).
6. G. Wang, K. Pran, G. Sagvolden, G. B. Havsgard, A. E. Jensen, G. A. Johnson, and S. T. Vohra, "Ship hull structure monitoring using fibre optic sensors," Smart Mater. Struct. **10**(3), 472–478 (2001).
7. H. P. Wang, P. Xiang, and L. Z. Jiang, "Optical fiber sensor based in-field structural performance monitoring of multilayered asphalt pavement," J. Lightwave Technol. **36**(17), 3624–3632 (2018).
8. H. P. Wang, L. Z. Jiang, and P. Xiang, "Priority design parameters of industrialized optical fiber sensors in civil engineering," Opt. Laser Technol. **100**, 119–128 (2018).
9. F. Z. Tan, Z. Y. Liu, J. J. Tu, C. Y. Yu, C. Lu, and H. Y. Tam, "Torsion sensor based on inter-core mode coupling in seven-core fiber," Opt. Express **26**(16), 19835–19844 (2018).
10. V. Budinski and D. Donlagic, "Fiber-optic sensors for measurements of torsion, twist and rotation: a review," Sensors **17**(3), 443 (2017).
11. B. Huang and X. W. Shu, "Ultra-compact strain- and temperature-insensitive torsion sensor based on a line-by-line inscribed phase-shifted FBG," Opt. Express **24**(16), 17670–17679 (2016).
12. B. Yin, H. S. Li, S. C. Feng, Y. L. Bai, Z. B. Liu, W. J. Peng, S. Liu, and S. S. Jian, "Temperature-independent and strain-independent twist sensor based on structured PM-CFBG," IEEE Photonics Technol. Lett. **26**(15), 1565–1568 (2014).
13. Y. P. Wang and Y. J. Rao, "Long period fibre grating torsion sensor measuring twist rate and determining twist direction simultaneously," Electron. Lett. **40**(3), 164–166 (2004).
14. L. Zhang, Y. Q. Liu, Y. H. Zhao, and T. Y. Wang, "High sensitivity twist sensor based on helical long-period grating written in two-mode fiber," IEEE Photonics Technol. Lett. **28**(15), 1629–1632 (2016).
15. R. Subramanian, C. L. Zhu, H. Zhao, and H. P. Li, "Torsion, strain, and temperature sensor based on helical long-period fiber gratings," IEEE Photonics Technol. Lett. **30**(4), 327–330 (2018).
16. D. J. Liu, R. Kumar, F. F. Wei, W. Han, A. K. Mallik, J. H. Yuan, C. X. Yu, Z. Kang, F. Li, Z. Y. Liu, H. Y. Tam, G. Farrell, Y. Semenova, and Q. Wu, "Highly sensitive twist sensor based on partially silver coated hollow core fiber structure," J. Lightwave Technol. **36**(17), 3672–3677 (2018).
17. Q. J. Fu, J. D. Zhang, C. C. Liang, I. P. Ikechukwu, G. L. Yin, L. Lu, Y. F. Shao, L. Liu, and T. Zhu, "Intensity-modulated directional torsion sensor based on in-line optical fiber Mach-Zehnder interferometer," Opt. Lett. **43**(10), 2414–2417 (2018).

Optical Materials EXPRESS

18. W. J. Ni, P. Lu, D. M. Liu, J. S. Zhang, and S. B. Jiang, "A highly sensitive twist sensor without temperature cross sensitivity based on tapered single-thin-single fiber offset structure," Proc. SPIE **10323**, 103235D (2017).
19. F. Zhang, S. Liu, Y. Wang, Y. J. Huang, X. Z. Xu, C. L. Fu, T. S. Wu, C. R. Liao, and Y. P. Wang, "Highly sensitive torsion sensor based on directional coupling in twisted photonic crystal fiber," Appl. Phys. Express **11**(4), 042501 (2018).
20. X. X. Kang, W. G. Zhang, Y. X. Zhang, J. Yang, L. Chen, L. X. Kong, Y. S. Zhang, L. Yu, T. Y. Yan, and P. C. Geng, "Intensity-demodulated torsion sensor based on thin-core polarization-maintaining fiber," Appl. Opt. **57**(13), 3474–3478 (2018).
21. H. L. Zhang, Z. F. Wu, P. P. Shum, X. G. Shao, R. X. Wang, X. Q. Dinh, S. N. Fu, W. J. Tong, and M. Tang, "Directional torsion and temperature discrimination based on a multicore fiber with a helical structure," Opt. Express **26**(1), 544–551 (2018).
22. Z. Y. Bai, M. Deng, S. Liu, Z. Zhang, J. S. Xu, J. Tang, Y. Wang, C. R. Liao, and Y. P. Wang, "Torsion sensor with rotation direction discrimination based on a pre-twisted in-fiber Mach-Zehnder Interferometer," IEEE Photonics J. **9**(3), 1–8 (2017).
23. S. J. Duan, W. L. Liu, C. T. Sun, H. Jiang, C. Yao, K. Zhang, X. Y. Bai, W. Wang, C. L. Lu, T. Geng, F. Peng, and L. B. Yuan, "High Sensitive Directional Twist Sensor Based on a Mach-Zehnder Interferometer," IEEE Photonics J. **10**(6), 1–7 (2018).
24. T. Zhu, Y. J. Rao, and Q. J. Mo, "A high sensitivity fiber-optic torsion sensor based on a novel ultra long-period fiber grating," Opt. Commun. **266**(1), 187–190 (2006).
25. B. Ibarra-Escamilla, E. A. Kuzin, F. Gutierrez-Zainos, R. Tellez-Garcia, J. W. Haus, R. Rojas-Laguna, and J. M. Estudillo-Ayala, "Measurement of beat length in short low-birefringence fibers using the fiber optical loop mirror," Opt. Commun. **217**(1-6), 211–219 (2003).
26. S. N. Khan, S. K. Chatterjee, and P. R. Chaudhuri, "Single all-optical platform for measurement of twist and transverse stress using polarization modulation in distinct dual-mode fiber placed in a Sagnac loop," J. Opt. Soc. Am. A **33**(1), 131–140 (2016).
27. X. Y. Liu, F. Fang, B. Sun, and Z. X. Zhang, "Twist sensor based on tapered few-mode fiber," Opt. Commun. **408**, 26–30 (2018).
28. B. Huang and X. W. Shu, "Highly Sensitive Twist Sensor Based on Temperature-and Strain-Independent Fiber Lyot Filter," J. Lightwave Technol. **35**(10), 2026–2031 (2017).
29. Y. H. Qian, B. Sun, H. D. Wan, and Z. X. Zhang, "Novel temperature-independent microfiber sensor fabricated with the tapering-twisting-tapering technique," Appl. Opt. **58**(12), 3091–3096 (2019).
30. J. Zubia, J. Arrue, and A. J. O. F. T. Mendioroz, "Theoretical analysis of the torsion-induced optical effect in a plastic optical fiber," Opt. Fiber Technol. **3**(2), 162–167 (1997).
31. Y. P. Wang, J. P. Chen, and Y. J. Rao, "Torsion characteristics of long-period fiber gratings induced by high-frequency CO_2 laser pulses," J. Opt. Soc. Am. B **22**(6), 1167–1172 (2005).
32. C. Li, S.-J. Qiu, Y. Chen, F. Xu, and Y.-Q. Lu, "Ultra-sensitive refractive index sensor with slightly tapered photonic crystal fiber," IEEE Photonics Technol. Lett. **24**(19), 1771–1774 (2012).
33. R. Yang, Y.-S. Yu, C. Chen, Y. Xue, X.-L. Zhang, J.-C. Guo, C. Wang, F. Zhu, B.-L. Zhang, Q.-D. Chen, and H.-B. Sun, "S-tapered fiber sensors for highly sensitive measurement of refractive index and axial strain," J. Lightwave Technol. **30**(19), 3126–3132 (2012).
34. G. Fu, Y. Li, X. Fu, W. Jin, and W. Bi, "Temperature insensitive curvature sensor based on cascading photonic crystal fiber," Opt. Fiber Technol. **41**, 64–68 (2018).